Environment International 176 (2023) 107967

Contents lists available at ScienceDirect

Environment International

journal homepage: www.elsevier.com/locate/envint

Full length article

Mortality burden due to ambient nitrogen dioxide pollution in China: Application of high-resolution models

Xinyue Li [a,1], Peng Wang [b,1], Weidong Wang [a], Hongliang Zhang [b], Su Shi [a], Tao Xue [c], Jintai Lin [d], Yuhang Zhang [d], Mengyao Liu [d], Renjie Chen [a], Haidong Kan [a], Xia Meng [a,e,*]

[a] School of Public Health, Key Laboratory of Public Health Safety of the Ministry of Education and Key Laboratory of Health Technology Assessment of the Ministry of Health, Fudan University, Shanghai 200302, China
[b] Department of Atmospheric and Oceanic Sciences, Fudan University, Shanghai 200438, China
[c] Institute of Reproductive and Child Health/National Health Commission Key Laboratory of Reproductive Health and Department of Epidemiology and Biostatistics, School of Public Health, Peking University Health Science Centre, Beijing, China
[d] Laboratory for Climate and Ocean-Atmosphere Studies, Department of Atmospheric and Oceanic Sciences, School of Physics, Peking University, Beijing 100871, China
[e] Shanghai Typhoon Institute/CMA, Shanghai Key Laboratory of Meteorology and Health, Shanghai 200030, China

ARTICLE INFO

Handling Editor: Adrian Covaci

Keywords:
Nitrogen dioxide
NO_2 column density
Mortality burden
Air quality guidelines

ABSTRACT

Background: A large gap exists between the latest Global Air Quality Guidelines (AQG 2021) and Chinese air quality standards for NO_2. Assessing whether and to what extent air quality standards for NO_2 should be tightened in China requires a comprehensive understanding of the spatiotemporal characteristics of population exposure to ambient NO_2 and related health risks, which have not been studied to date.
Objective: We predicted ground NO_2 concentrations with high resolution in mainland China, explored exposure characteristics to NO_2 pollution, and assessed the mortality burden attributable to NO_2 exposure.
Methods: Daily NO_2 concentrations in 2019 were predicted at 1-km spatial resolution in mainland China using random forest models incorporating multiple predictors. From these high-resolution predictions, we explored the spatiotemporal distribution of NO_2, population and area percentages with NO_2 exposure exceeding criterion levels, and premature deaths attributable to long- and short-term NO_2 exposure in China.
Results: The cross-validation R^2 and root mean squared error of the NO_2 predicting model were 0.80 and 7.78 μg/m^3, respectively, at the daily level in 2019. The percentage of people (population number) with annual NO_2 exposure over 40 μg/m^3 in mainland China in 2019 was 10.40 % (145,605,200), and it reached 99.68 % (1,395,569,840) with the AQG guideline value of 10 μg/m^3. NO_2 levels and population exposure risk were elevated in urban areas than in rural. Long- and short-term exposures to NO_2 were associated with 285,036 and 121,263 non-accidental deaths, respectively, in China in 2019. Tightening standards in steps gradually would increase the potential health benefit.
Conclusion: In China, NO_2 pollution is associated with significant mortality burden. Spatial disparities exist in NO_2 pollution and exposure risks. China's current air quality standards may no longer objectively reflect the severity of NO_2 pollution and exposure risk. Tightening the national standards for NO_2 is needed and will lead to significant health benefits.

1. Introduction

Nitrogen dioxide (NO_2) is a major ambient air pollutant that is hazardous to public health. Previous health studies have reported adverse effects of NO_2 on multiple health outcomes, including mortality and morbidity from non-accidental diseases as well as respiratory and cardiovascular diseases (Achakulwisut et al. 2019; Kaufman et al. 2016; Zhang et al. 2018). For example, a global study found that short-term exposure to 10 μg /m^3 increment of NO_2 was associated with an increase of 0.46 % in total mortality, and the association was nearly linear,

* Corresponding author at: School of Public Health, Key Laboratory of Public Health Safety of the Ministry of Education and Key Laboratory of Health Technology Assessment of the Ministry of Health, Fudan University, Shanghai 200032, China.
E-mail address: mengxia@fudan.edu.cn (X. Meng).
[1] Xinyue Li and Peng Wang contributed equally to this work.

https://doi.org/10.1016/j.envint.2023.107967
Received 13 December 2022; Received in revised form 7 April 2023; Accepted 7 May 2023
Available online 12 May 2023

with no discernible threshold (Meng et al., 2021a). Evidence from cohort studies and recent meta-analyses support these adverse associations between long-term NO_2 exposure and mortality(Atkinson et al. 2018; Huang et al. 2021; Huangfu and Atkinson 2020; Mills et al. 2015). After adjusting for the effects of other pollutants (e.g., fine particulate matter [$PM_{2.5}$] and ozone), the associations between NO_2 and health outcomes in many studies remained robust, reflecting the independent health effects of NO_2 (Huang et al. 2021; Meng et al., 2021a; Mills et al. 2015).

Based on evidence from health studies and systematic reviews conducted in the past few years, the World Health Organization (WHO) launched the Global Air Quality Guidelines in 2021 (AQG 2021), in which the guideline value for NO_2 at the annual level was strengthened from 40 μg/m^3 to 10 μg/m^3 and a 24-h guideline value of 25 μg/m^3 was added for NO_2 compared to the previous Air Quality Guidelines launched in 2005 (World Health Organization, 2005; World Health Organization, 2021). A large gap exists between the latest WHO guideline values and current air quality standards in China for NO_2, with the latter including annual and 24 h average standards for NO_2 of 40 μg/m^3 and 80 μg/m^3, respectively (Chinese Ministry of Environmental Protection, 2012). Assessing whether and to what extent the air quality standards for NO_2 in China should be tightened requires a comprehensive understanding of the spatiotemporal characteristics of population exposure to ambient NO_2 and associated health risks, which have not been studied to date.

Strong spatial gradients of local variability of ambient NO_2 concentrations have been reported in previous studies (Cyrys et al. 2012; Gurung et al. 2017), as NO_2 concentrations decay sharply with increasing distance from anthropogenic emission sources. The distribution of NO_2 shows spatially disparities due to its relatively short lifetime and various emission sources. The emission patterns of NO_2 also lead to urban–rural disparities, with higher traffic-related NO_2 emissions in urban areas than rural areas (Anenberg et al. 2022). These characteristics of NO_2 complicate accurate exposure assessment based on fixed monitoring stations. Because fixed stations are of limited numbers and unevenly distributed, measurements from them could not fully represent the spatiotemporal variation of ambient NO_2 levels and related exposure levels in areas without stations. The exposure error may impact the accuracy of NO_2-related health estimates (Xiao et al. 2018).

For these reasons, modeling approaches are widely employed in epidemiological studies to improve the resolution and accuracy of NO_2 exposure assessment. Traditional geospatial statistical methods, represented by land-use regression (LUR) models, are good at capturing the spatial variation in NO_2 at high resolution (Xu et al., 2019; Young et al. 2016). However, due to the limited update frequency of major predictor variables, traditional geospatial statistical methods generally cannot capture subtle temporal changes in exposure. The application of remote sensing data to model development has helped to extend both the spatial and temporal resolutions of NO_2 predictions (Xu et al., 2019; Yang et al. 2017). Previous studies have mainly relied on column NO_2 density data from the Ozone Measuring Instrument (OMI) aboard the Aura satellite for NO_2 modeling. However, this data has a relatively low spatial-resolution and a high missing rate due to technical issues. Since 2018, satellite retrievals from the TROPOspheric Monitoring Instrument (TROPOMI) have become available with higher spatiotemporal resolution of 3.5 km × 7 km and less missing data. We found that column NO_2 density data from TROPOMI better represents ground-level NO_2 variation than data from OMI (Iqbal et al. 2022; Wang et al. 2020). The use of TROPOMI NO_2 data remains limited in China, which has the highest NO_2 pollution levels worldwide (Li and Wu 2021; Liu 2021).

Therefore, in this study, we developed models based on the random forest algorithm incorporating satellite retrievals from TROPOMI to predict ground NO_2 concentrations with full spatiotemporal coverage at daily level and 1 km × 1 km resolution in mainland China; used the high-resolution predictions to evaluate the spatiotemporal patterns of NO_2 pollution levels, population exposure characteristics, and urban/rural disparity of NO_2 pollution according to guideline values in the WHO AQG 2021 (World Health Organization, 2021) and current air quality standards of China; and assessed the mortality burdens associated with long-term and short-term exposure to NO_2 in China and potential health benefits associated with decreasing NO_2 levels in the future.

2. Data and methods

2.1. Data

Data from 2019 were collected, reprojected and integrated in this study. We selected 2019 because it was the latest year that was not affected by the COVID-19 pandemic and lockdown policies in China in recent years, which reduced NO_2 concentrations compared to previous periods (Sannigrahi et al. 2021). We first constructed a grid of 1 km × 1 km spatial resolution covering the mainland of China based on the sinusoidal projection with geographic coordinate of WGS84, which is the same with developing models for $PM_{2.5}$ and ozone (Meng et al. 2022; Shi et al. 2023). Then, the spatial datasets of different variables were all reprojected to sinusoidal projection, if they are not. Finally, all data were integrated into the 1-km grid with methods of spatial joining or inverse distance weighting (IDW) interpolation.

2.1.1. Ground measurements of NO_2 concentrations

The National Air Quality Monitoring Network in mainland China was established in 2013 and monitoring data have been published at https://www.cnemc.cn/ since then. Hourly NO_2 concentrations at 1546 ground monitoring stations in 2019 were collected to calculate daily mean NO_2 concentrations from at least 18 valid hourly measurements. During data processing, ground measurement of NO_2 concentrations over detection limits (1026 μg/m^3) and observations with the same values for at least 8 continuous hours were removed (Wu et al. 2018). Monitoring stations were spatially joined with the 1 -km grid and mean NO_2 concentrations were calculated to present the average pollution levels within the cell if multiple stations fell into it.

2.1.2. Satellite-derived NO_2 column density

The TROPOMI instrument onboard the Sentinel-5 Precursor (S5P) satellite was launched in October 2017 and TROPOMI tropospheric NO_2 vertical column density (VCD) products have been available since July 2018. Based on TROPOMI NO_2 VCD, the Atmospheric Chemistry and Modelling Group of Peking University developed the POMINO-TROPOMI product (https://www.pku-atmos-acm.org/), which was applied in our study. The POMINO-TROPOMI product considers aerosol optical effects and their vertical profiles, angular dependence of surface reflectance, and dynamically variable atmospheric profiles of air pressure, air temperature and NO_2 at a high horizontal resolution (about 25 km). Therefore, this product captures the spatiotemporal variation in NO_2 well and reduces the systematic sampling bias in heavy pollution situations (Lin et al. 2015; Liu et al. 2020). Daily tropospheric NO_2 VCD from POMINO-TROPOMI version-1 level-3 data with 0.05° × 0.05° spatial resolution was downloaded, reprojected and interpolated into the 1 km grid using the IDW method.

2.1.3. NO_2 simulation from community multiscale air quality (CMAQ)

Ground-level NO_2 concentrations simulated by the CMAQ model version 5.0.2 were applied in the model(Ying et al. 2015), with meteorological inputs generated from the Weather Research and Forecasting (WRF) model version 4.2.2. NO_2 simulations produced by CMAQ were re-estimated at the 1km grid using IDW. The CMAQ model had a horizontal resolution of 36 km and covered all land areas in and around China, and the detail of the domain was described in (Wang et al. 2018). The model initial and boundary conditions were taken from the default CMAQ model. The anthropogenic emissions were from the Emission Database for Global Atmospheric Research (EDGAR) version 5.0 (https://edgar.jrc.ec.europa.eu/, last accessed: 04 Nov. 2022). For input

factor in CMAQ model, biogenic and wildfire emissions were generated using the Model of Emissions of Gases and aerosols from Nature (MEGAN) v2.1(Guenther et al. 2012) and the Fire Inventory from NCAR (FINN) (Wiedinmyer et al. 2011), respectively.

2.1.4. Meteorological parameters

Meteorological parameters for 2019 were extracted from GEOS 5-FP (the Goddard Earth Observing System Data Assimilation System GEOS-5 Forward Processing) at 0.25° × 0.3125° resolution (NASA 2013). The parameters of air temperature and relative humidity at 2 m, total precipitation, wind speed at 10 m, surface pressure, total cloud fraction, and planetary boundary layer height (PBLH) were included in this study. The meteorological parameters were interpolated to the 1-km grid cells using the IDW method and matched with NO_2 measurements at the daily level. Precipitation and PBLH on the previous day were also included (NASA 2013).

2.1.5. Other predictor variables

Ancillary variables included elevation, population, road networks and land cover. Elevation data were extracted from the Advanced Spaceborne Thermal Emission and Reflection Radiometer (ASTER) Global Digital Elevation Map (GDEM) at 30 m spatial resolution (National Aeronautics and Space Administration 2019), and were averaged within the 1-km grid cells. Population data from the LandScan Global Population Database (https://landscan.ornl.gov/) were aligned with the 1 km grid cells using IDW method. Road length, defined as the total length of all road types within a 1 km grid cell, was calculated. Normalized Difference Vegetation Index (NDVI) values at 1 km resolution obtained from the MODIS 16-day NDVI product (MOD13A2) were spatially joined to the grid (Land Processes Distributed Active Archive Center 2021).

2.1.6. Urban/rural classification

Land-cover classification data of urban/rural regions at 30 m resolution were downloaded from https://data.ess.tsinghua.edu.cn/ for use in this analysis (Gong et al. 2019; Gong et al. 2019b). We assigned each 1-km grid cell as either urban or rural according to the majority of the 30 m urban/rural grid cells.

2.1.7. Baseline mortality

The annual baseline mortalities and populations of urban and rural areas in 2019 were obtained from the China Health Statistics Yearbook 2020 published by National Health Commission of China and the China Statistical Yearbook 2020 published by the National Bureau of Statistics of China, separately. The nationwide annual non-accidental mortality rate was calculated by weighting the populations and non-accidental mortality rates in rural and urban areas. After obtaining nationwide annual non-accidental mortality, we used the percentage of deaths nationwide per month from the National Population Census (https://www.stats.gov.cn/) to calculate monthly mortality, and daily mean mortality rate was calculated by dividing the monthly mortality by the number of days in the corresponding month to calculate deaths attributable to short-term NO_2 exposure.

2.2. Methods

2.2.1. Model development

Ground NO_2 measurements were used as the dependent variable and all variables described above, including POMINO-TROPOMI NO_2 VCD, CMAQ simulated NO_2 concentrations, meteorological data, elevation, population, road networks, and NDVI, were used as predictor variables to train the random forest model (satellite model). A second model (non-satellite model) was established with the same ancillary predictors except satellite retrievals. Predictions with full spatiotemporal coverage were produced using predictions from the satellite model for grid cells and days with available satellite NO_2 VCD and predictions from the non-satellite model where NO_2 VCD were missing. This method has been used to fill the gap in predictions of air pollutants led by missingness of satellite data in previous studies (Meng et al. 2021b; Xiao et al. 2021).

Cross-validation (CV) was conducted to indicate the predictive accuracy and test for overfitting of the models. In addition to the standard 10-fold CV, we also performed temporal and spatial CV to evaluate model performance at temporal and spatial extrapolation. For 10-fold temporal CV, a training model was developed using data from a randomly selected 90% of days to predict NO_2 concentrations on the remaining 10% of days, and this process was repeated 10 times. Similarly, 10-fold spatial CV was conducted at each time using a training model with data randomly selected from 90% of stations to make predictions for the remaining 10% of stations. The regression R^2, intercept, slope, root mean square error (RMSE), and mean absolute percentage error (MAPE) values were calculated between NO_2 measurements and NO_2 predictions for CV (Li et al. 2022). RMSE was calculated as the square root of the average of the squared differences between the predicted and observed values. MAPE was percentage calculated by using the absolute difference between the predicted and observed values and dividing it by the observed values. In addition, we explored the variation of prediction performance by season and region to better display the performance of models.

The spatiotemporal characteristics and population exposure levels were analyzed based on NO_2 predictions as well as AQG criteria and the Chinese air quality standard for NO_2. First, the spatial distributions and temporal trends were evaluated based on NO_2 predictions in mainland China. Second, the percentages of the total population and area with NO_2 levels exceeding the AQG criteria and national standard were assessed. AQG 2021 set interim targets (ITs) and guideline values of 40 μg/m^3, 30 μg/m^3, 20 μg/m^3, and 10 μg/m^3 for long-term NO_2 exposure, and 120 μg/m^3, 50 μg/m^3, and 25 μg/m^3 for short-term NO_2 exposure (World Health Organization, 2021). China has set air quality standards of 40 μg/m^3 and 80 μg/m^3 for long-term and short-term exposure, respectively (Ministry of Ecology and Environnmental of the People's Republic of China, 2012).

2.2.2. Long-term and short-term NO_2 exposure-related mortality burdens

First, we calculated attributable deaths for long-term and short-term NO_2 exposure under current pollution level. Then, we calculated preventable deaths, assuming that NO_2 concentrations could reach different NO_2 criteria in the future. The formulas were showed as follows, with attributable death and preventable death differing mainly in the selection of counterfactual concentrations.

Deaths related to long-term NO_2 exposure were calculated following equations (1) - (4) (Cohen et al. 2017; Meng et al. 2023):

$$RR_i = e^{\beta(x_i - x_{cf})} \quad (1)$$

where RR_i is the relative risk value of grid cell i; β is the pooled effect estimate of long-term NO_2 exposure on total non-accidental deaths calculated in a meta-analysis based on 41 cohort studies worldwide, with a value of 0.0020 (95 %CI: 0.0010, 0.0039) (Huangfu and Atkinson 2020); x_i is the estimated NO_2 concentration in grid cell i; x_{cf} is the counterfactual concentration suggested in AQG 2021 as the starting point for deriving a long-term guideline value, which is 8.8 μg/m^3 (World Health Organization, 2021);

$$paf_i = \frac{RR_i - 1}{RR_i} \quad (2)$$

$$PAF = 1 - 1/\frac{\Sigma POP_i * \left(\frac{1}{1-paf_i}\right)}{\Sigma POP_i} \quad (3)$$

where paf_i is the population attributable fraction of non-accidental death in grid cell i; PAF is the overall population attributable fraction in the whole study domain; POP_i is the population in grid cell i;

$$Attributable\ \ Death = PAF \times POP \times Mortality \quad (4)$$

where *Attributable Death* is the total attributable death in mainland China; *POP* is the total population in 2019 reported by the China Statistical Bureau; and *Mortality* is the nationwide non-accidental mortality in 2019 calculated as described in section 2.1.7. Based on the reported 95 % CI for the RR, the uncertainty ranges were calculated for the corresponding estimates of PAFs and attributable deaths. PAF values in urban and rural areas and each province were also calculated separately using equation (1) - (3), to explore the spatial disparity of NO_2 related health risks.

For short-term NO_2 exposure, premature deaths attributable to NO_2 were also assessed using equations (1)– (4). The differences in this analysis are that β is the pooled health effect calculated from a study conducted in 272 cities in China, with a value of 0.0009 (95 % CI: 0.0007, 0.0011) (Chen et al. 2018); x_{cf} is the counterfactual concentration suggested in AQG 2021 as the starting point for deriving the short-term guideline value, which is 10 μg/m^3 (World Health Organization, 2021); and *Mortality* is the daily non-accidental mortality in 2019 calculated as described in section 2.1.7. The daily attributable deaths nationwide were calculated first and then summed to obtain the total attributable deaths in 2019.

For cause-specific death, deaths attributable to respiratory diseases for long-term and short-term NO_2 exposure were calculated in the same way with RR values from the above literature (Chen et al. 2018; Huangfu and Atkinson 2020) and respiratory mortality data from the China Health Statistics Yearbook 2020.

For preventable death, it was calculated using various NO_2 criteria set as Its and guideline values for long-term and short-term NO_2 pollution in AQG 2021, and Chinese air quality standards as the counterfactual concentration.

3. Results

3.1. Model performance

Approximately 500,062 NO_2 measurements collected from 1,546 monitoring stations in 2019 were used for model development, and the station locations are shown in Figure S1. Based on NO_2 measurements, the daily mean (standard deviation) NO_2 concentration in 2019 was 29.34 (17.32) μg/m^3, with a range of 1.32 μg/m^3 to 156.96 μg/m^3. From the NO_2 predicting models, the daily mean (standard deviation) NO_2 concentration at the monitoring stations was 29.13 (14.25) μg/m^3, with a range of 2.67 μg/m^3 to 123.84 μg/m^3. The results of model CV are presented in Fig. 1. The density scatter plots indicate that most measurement–prediction pairs fell along the 1:1 line, indicating high consistency between measurements and predictions. For combined predictions from the two models, the overall, temporal and spatial CV R^2 (RMSE) values were 0.80 (7.78 μg/m^3), 0.69 (9.74 μg/m^3) and 0.73 (9.00 μg/m^3), respectively. CV results of the combined model broken up by region and season were shown in Figure S2 and Figure S3. The model performance was similar between regions with CV R^2 of 0.78 – 0.84 and RMSE of 6.41 – 8.49 μg/m^3. The predicting accuracy was slightly different among seasons, which was higher in winter and autumn.

The results of CV for satellite model and non-satellite model were comparable, with R^2 of 0.79 for the satellite model and 0.81 for the non-satellite model, but the two models had their own advantages and limitations. For satellite model, it was better at capturing the variation of NO_2 pollution. As shown in Figure S5, predictions from satellite model captured higher concentrations of NO_2 and contrast between urban and rural areas. However, missingness of satellite data was high and occurred non-randomly (Table S1), which could bias the predictions at monthly and annual levels. For example, predictions derived from the satellite model tended to overestimate NO_2 concentrations in winter in Central and East China, but underestimate NO_2 concentrations in spring in South China. Non-satellite model could provide full spatiotemporal-coverage predictions, though was not as good as satellite model in capturing high spatial-variability of NO_2 concentrations. Therefore, the combination of the two models could improve both the accuracy and the coverage of the predictions.

Importance rankings of predictors produced by the satellite model and non-satellite model are shown in Figure S4. For the satellite model, TROPOMI NO_2 VCD was the most important predictor, followed by NO_2 estimates from CMAQ. For the non-satellite model, the NO_2 estimate from CMAQ was the most important predictor. The predictors with high ranks for both models were total precipitation on the previous day, humidity at 2 m, wind at 10 m, surface pressure and elevation.

3.2. Spatiotemporal characteristics of NO_2 pollution

Temporally, as shown in Fig. 2(A), NO_2 concentrations showed significant seasonal trends, with higher levels in winter (18.54 μg/m^3) than in summer (12.71 μg/m^3) based on NO_2 predictions across all grid cells. According to the 24 h NO_2 concentration guideline value (25 μg/m^3) recommended in AQG 2021, the months with the highest percentage of grid-days exceeding this criterion were from November to January (Table S2), ranging from 14.44 % to 17.79 %; while the lowest percentages were observed from June to August, ranging from 1.21 % to 2.61 %. Extreme NO_2 pollution exceeding IT-1 (120 μg/m^3) of AQG 2021 or the Chinese air quality standard (80 μg/m^3) occurred only between October and March (0.002–0.062 %). Light to moderate NO_2 pollution exceeding IT-2 (50 μg/m^3) occurred in all months (0.001–2.257 %). Daily NO_2 concentrations exceeded the WHO guideline value (25 μg/m^3) in more than 8% of all grid-days, while 0.01 % of grid-days exceeded the Chinese air quality standard (80 μg/m^3).

Spatially, the annual average NO_2 concentrations in 2019 were unevenly distributed nationwide, which were consistent with the spatial distributions of population density and road networks, as shown in Fig. 2

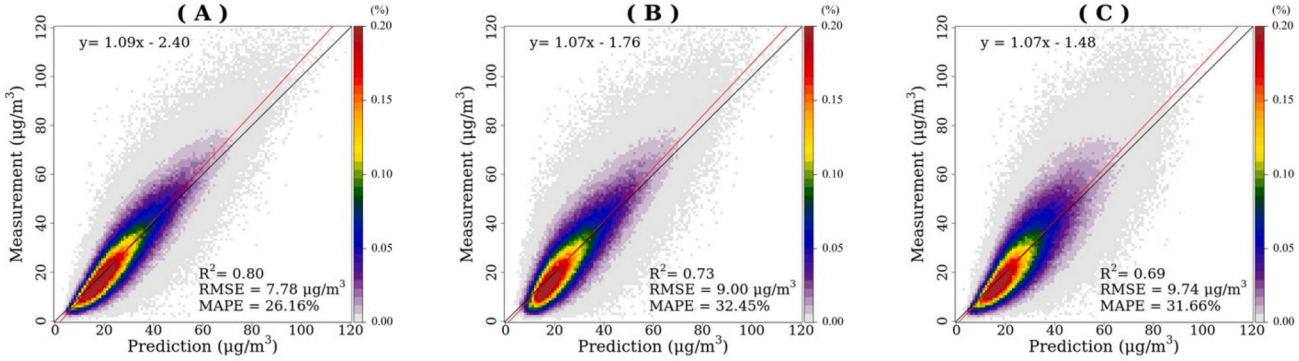

Fig. 1. Density scatter plots and linear regressions between ground NO_2 measurements and NO_2 predictions obtained from the combined random forest models in 2019. (A) Overall CV; (B) spatial CV; (C) temporal CV. Black line: 1:1 line; red line: regression line. (For interpretation of the references to colour in this figure legend, the reader is referred to the web version of this article.)

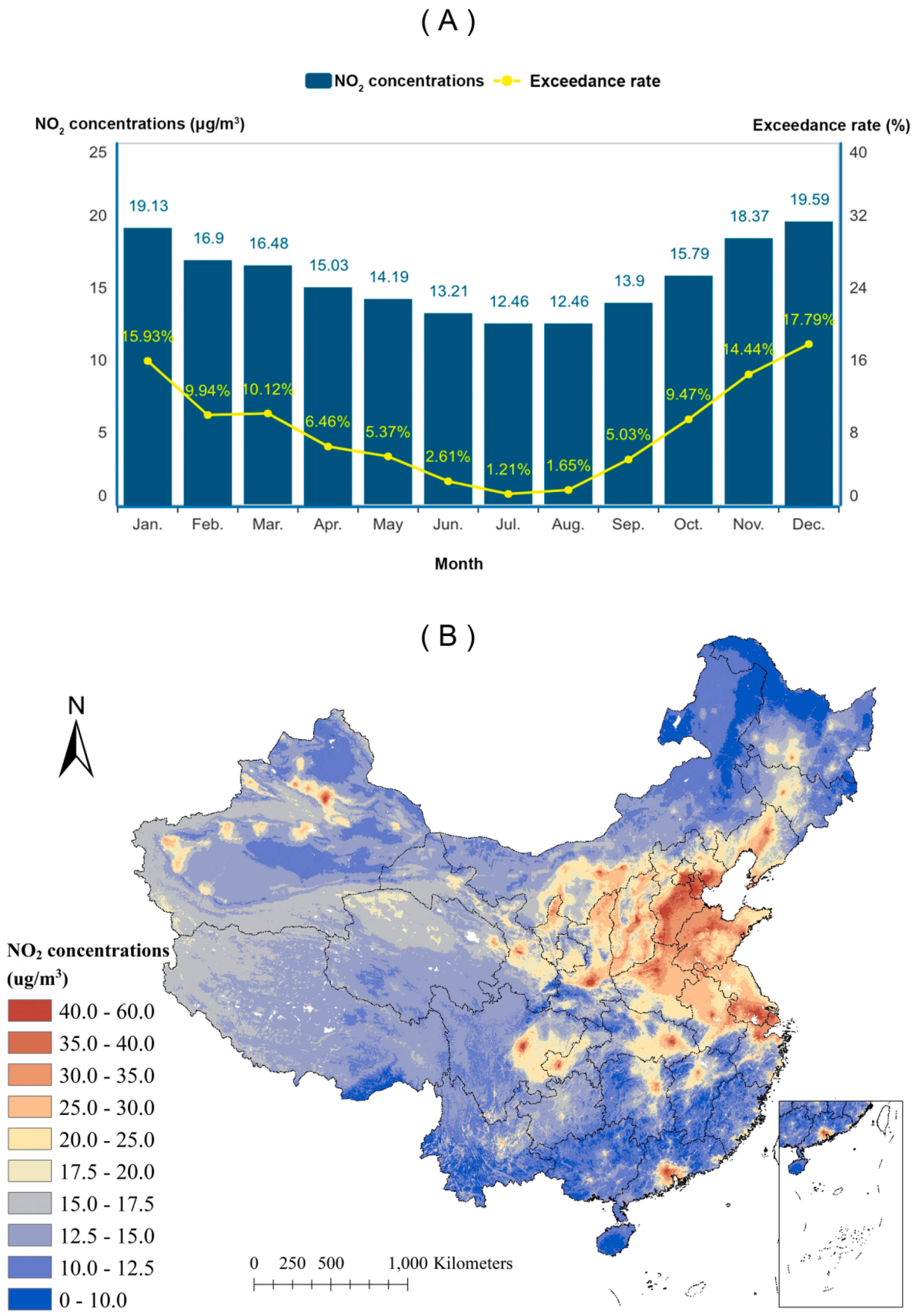

Fig. 2. Spatiotemporal distribution of annual mean NO_2 concentrations across mainland China in 2019. (A) Monthly mean NO_2 concentrations (left Y-axis) and exceedance rates of daily NO_2 concentrations in each month (right Y-axis) according to the guideline value (25 μg/m^3) for daily NO_2 concentrations in AQG 2021; (B) spatial distribution of annual mean NO_2 concentrations at 1 km × 1 km spatial resolution in 2019.

(B) and Figure S6. Based on full-coverage NO_2 predictions, the annual mean (standard deviation) NO_2 concentration of all grids nationwide was 15.63 (5.58) μg/m^3, with a range of 5.60 μg/m^3 to 69.92 μg/m^3. Overall, NO_2 concentrations were high in central and eastern China, and low in western China. In addition, NO_2 concentrations were high in city clusters, such as Beijing–Tianjin–Hebei, the Yangtze River Delta, and the Pearl River Delta, as well as major cities in each province. Several cities in Xinjiang Province, western China, had elevated NO_2 concentrations, indicating the path of the Silk Road. In addition, differences were found in the distribution of NO_2 concentrations between rural and urban areas. In 2019, the annual average NO_2 concentration was 27.94 μg/m^3 in urban areas and 15.50 μg/m^3 in rural areas (Fig. 3(A)).

The national annual population-weighted NO_2 concentration was 25.82 μg/m^3, higher than annual mean NO_2 concentration of 15.63 μg/m^3, indicating that more people lived in areas with higher NO_2 concentrations. The area proportion and population proportion living in areas exceeding different criteria and standards were calculated nationwide and in urban and rural areas separately, and the results are shown in Fig. 3(B). Regardless of the criteria or standards used, the percentages of population exposed to NO_2 in excess of the criteria or standard were consistently higher than the corresponding percentages in terms of area. Based on the guideline value (10 μg/m^3) for annual mean NO_2 concentrations recommended in AQG 2021, only 7.10 % of the area of mainland China met this criterion in 2019, representing a population proportion of only 0.32 %. However, according to the Chinese air quality standard, which is equivalent to the WHO AQG of IT-1 (40 μg/m^3), most of the area and population met the standard, with only 0.42 % of the total area and 10.40 % of the total population exposed to NO_2 concentrations exceeding the standard.

In addition, the percentages of area and population exposed to annual mean NO_2 concentrations exceeding various criteria or standards were consistently higher in urban areas than in rural areas, suggesting that the population in urban areas was at higher risk of exposure to NO_2 pollution than people living in rural areas. For example, based on the guideline value of 10 μg/m^3, the proportions of total area meeting this criterion were 7.25 % of rural areas and 0.14 % of urban areas, while the impacted proportions of the population were 0.44 % and 0.09 % in rural and urban areas, respectively.

3.3. Long-term and short-term NO_2 pollution-related mortality burdens

3.3.1. Long-term NO_2 pollution-related mortality burdens

In China, the total PAF was 0.033 in 2019, indicating that 3.3 % of total mortality was attributable to NO_2 pollution. In the spatial distribution of PAFs at both grid and provincial levels, higher correlation with population density and spatial disparity of PAF were found, which was consistent with the distribution of population-weighted NO_2 concentration as shown in Fig. 4, Figure S7 and Figure S8. The gridded PAF values for long-term NO_2 exposure were higher in North China and East China, ranging from 0.019 to 0.065, and lower in Southwest China, ranging from 0.010 to 0.032. As shown in Fig. 4(C), the median PAF increased with increasing population, and the median PAF in grid cells with population higher than 10,000 was almost 5 times that in grid cells with population less than 10.

Based on NO_2 pollution levels in 2019, the number of deaths attributable to NO_2 pollution was 285,036 (95 % CI: 144,049, 558,139) for long-term exposure. Reducing NO_2 concentrations to the levels of IT-1 (40 μg/m^3), IT-2 (30 μg/m^3), IT-3 (20 μg/m^3) or the guideline value (10 μg/m^3) recommended in the WHO AQG 2021 could prevent 5,346 (95 % CI: 2,680, 10,633), 41,200 (95 % CI: 20,646, 82,035), 124,369 (95 % CI: 62,455, 246,596), and 265,394 (95 % CI: 134,018, 520,475) non-accidental deaths, respectively (Table 1). Among all non-accidental deaths attributable to long-term exposure, deaths attributable to respiratory disease were 47,633 (95 % CI: 16,219, 77,737)).

3.3.2. Short-term NO_2 pollution-related mortality burdens

Daily mean PAF of NO_2 in China was 0.014 in 2019, ranging from 0.005 to 0.030. Further, the monthly mean PAF of China ranged from 0.007 to 0.022, with lower values in summer and higher values in winter, which was consistent with the seasonal distribution of NO_2 concentrations. Based on the NO_2 pollution levels in 2019, the number of non-accidental deaths attributable to short-term NO_2 pollution exposure was 121,263 (95 % CI: 94,501, 147,921). Reducing the NO_2 concentration to IT-2 (50 μg/m^3) or the guideline value (25 μg/m^3) could prevent 5,337 (95 % CI: 4,149, 6,526) or 42,983 (95 % CI: 33,447, 52,509) non-accidental deaths, respectively (Table 1). Deaths attributable to respiratory disease were 18,152 (95 % CI: 13,654, 22,623) for short-term NO_2 exposure.

4. Discussion

We developed random forest models and predicted NO_2 concentrations at daily level and 1 km × 1 km spatial resolution with full spatiotemporal coverage of mainland China. Using those predictions, we found that the distribution of NO_2 was consistent with the locations of cities and road networks. A large proportion of the population of China was exposed to NO_2 concentrations exceeding the guideline value recommended by the WHO and an urban–rural disparity of exposure was observed. The numbers of deaths (95 % CI) attributable to long-term and short-term NO_2 exposure were 285,036 (144,049, 558,139) and 121,263 (94,501, 147,921), respectively, in mainland China in 2019. Thus, tightening of NO_2-related standards in the future would have major health benefits.

The NO_2 prediction models developed in this study have relatively

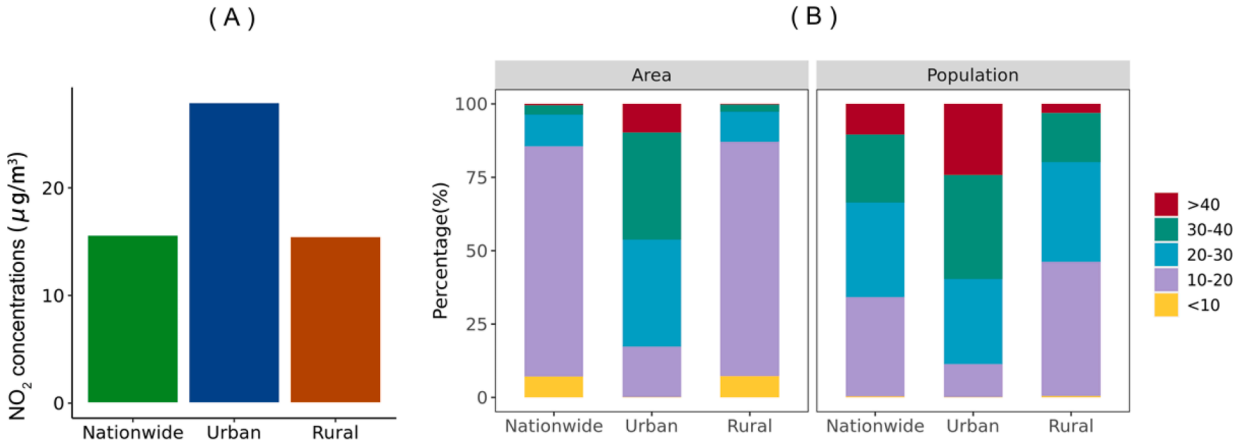

Fig. 3. Annual mean NO_2 concentrations (A) and exceedance rates in terms of area and population based on various criteria and standards (B) in China in 2019.

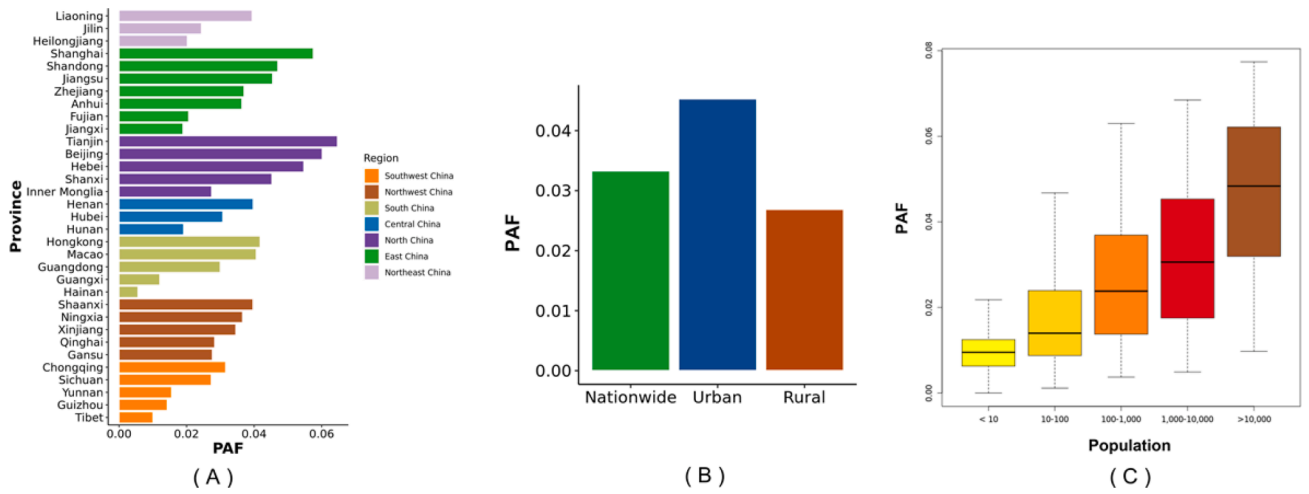

Fig. 4. Distribution of population attributable fraction for NO_2 long-term exposure in 2019. (A) Among provinces; (B) between urban and rural areas; and (C) in different population.

Table 1
Long-term and short-term preventable deaths if NO_2 concentrations in 2019 could be reduced to different lower levels.

Long-term NO_2 counterfactual concentration (ug/m^3)	National preventable deaths (95 %CI)	Short-term NO_2 counterfactual concentration (ug/m^3)	National preventable deaths (95 %CI)
40 (IT-1/ Chinese standard)	5,346 (2,680, 10,633)	120 (IT-1)	-*
30 (IT-1)	41,200 (20,646, 82,035)	80 (Chinese standard)	189 (147, 232)
20 (IT-3)	124,369 (62,455, 246,596)	50 (IT-2)	5,337 (4,149, 6,526)
10 (guideline value)	265,394 (134,018, 520,475)	25 (guideline value)	42,983 (33,447, 52,509)

* At the daily average level in 2019, there were no days with NO_2 concentrations above 120 ug/m^3, so related deaths were not calculated.

high accuracy and spatiotemporal resolution. In this study, the CV R^2 between measured and predicted NO_2 concentrations at the daily level was 0.80 in 2019. The RMSE and MAPE obtained from CV were 7.78 μg/m^3 and 26.16%, respectively. Several previous studies conducted in China have applied machine learning methods and satellite data to predict NO_2 concentrations, with R^2 ranging from 0.77 to 0.80 (Huang et al. 2022; Li et al. 2021; Zhu et al. 2019). Our study showed similar model performance to those studies, reflecting the reliability of the prediction model. In addition, previous studies often use satellite retrievals from OMI (Huang et al. 2022; Li et al. 2021; Li and Wu 2021), while few studies have yet applied TROPOMI data to model development. This study applied TROPOMI data, which have fewer missing data and higher spatial resolution than OMI data, to better capture the spatial variability of NO_2 at small scales (Wang et al. 2020). The combination of satellite and non-satellite models also improved both model performance and prediction coverage.

Based on the high-resolution NO_2 prediction model, we found that NO_2 concentrations in China had a marked seasonal trend and an uneven spatial distribution. NO_2 concentrations in China were lower in spring and summer and higher in autumn and winter. Higher NO_2 concentrations during cold seasons may be driven by the increased burning of fuels for heating (Wang et al. 2019). The seasonal trend is also influenced by weather conditions (Shen et al. 2021). Increased temperature and ideal diffusion conditions in spring and summer cause NO_2 concentrations to decrease. In terms of spatial distribution, NO_2 concentrations were highest in city clusters and areas with high densities of road networks and population, in accordance with NO_2 emissions from traffic, residential and industrial sources (Bechle et al. 2013; Zhang et al. 2013).

In addition to NO_2 concentrations, the PAF for NO_2 exposure was also higher in urban areas than in rural areas of China, indicating the disproportional exposure and health risks associated with NO_2 pollution. The United Nations estimates that by 2050, the global urbanization rate will increase to 68% from 56% in 2021 in demographic terms, with much of the population growth in urban areas concentrated in Asia and Africa, and China's urban population is expected to increase by 255 million from 2021 to 2050 (United Nations Human Settlements Programme 2022). In the context of rapid urbanization, increasing people are expected to expose to high levels of NO_2 pollution in China in the future. Moreover, emissions from transportation and anthropogenic activities would remain at relatively high levels, hindering the mitigation of NO_2 pollution in cities (Gan et al. 2021). The urban–rural disparity in NO_2 pollution levels and related exposure risks suggests that policymakers should consider the urbanization trend and synergistic relationship between increased population and air pollution levels when developing future measures to improve air quality.

A large gap exists between the air quality standard enacted in China and the WHO air quality guidelines for NO_2 regulation, and gradual strengthening of the Chinese air quality standard in the future could provide a great benefit to public health. The severity of NO_2 pollution differs among evaluation criteria. For example, 92.90% of the total area and 99.68% of the population were exposed to NO_2 concentrations higher than the AQG guideline value of 10 μg/m^3 in China in 2019, while the corresponding percentages were only 0.42% and 10.40%, respectively, based on the Chinese air quality standard of 40 μg/m^3. Deaths attributable to long-term NO_2 pollution numbered 285,036 in 2019, demonstrating a large amount mortality burden associated with high NO_2 concentrations in China. China has one of the highest NO_2 concentrations worldwide; thus, the current air quality standards do not objectively reflect the severity of NO_2 pollution and its exposure hazards to public health in China. Therefore, tightening of air quality standards and targeted efforts to decrease NO_2 concentrations and thereby protect public health are urgently needed.

Considering the current high NO_2 concentrations, tightening NO_2 standards in steps to progressively reduce air pollution in China is necessary. Previous studies have found a nearly linear association between short-term NO_2 pollution and mortality with no discernible thresholds, suggesting that any degree of reduction in NO_2 pollution will be protective for public health. We calculate that 5,346, 41,200, or

124,369 deaths could be prevented in the future if the annual mean NO_2 concentration were decreased to the IT-1 (40 μg/m^3), IT-2 (30 μg/m^3), or IT-3 (20 μg/m^3) levels recommended by the WHO in AQG 2021, respectively. Therefore, pollution reduction policies and air quality standards that are achievable within realistic time frames should be developed to improve air quality and provide health benefits in a stepwise manner in China, with the aim of ultimately meeting WHO air quality guidelines.

This study is subject to the following limitations. First, limited by data accessibility, high-resolution traffic flow and emissions data were not used in NO_2 model development. Instead, we used road length at 1-km resolution to indicate the contribution of transportation to NO_2 concentrations, in accordance with previous studies. We also included CMAQ-simulated NO_2 data, which was produced based on emissions and meteorological inputs. More effective predictors related to NO_2 pollution are needed to improve prediction accuracy in future studies. Second, the urban/rural classification data were from 2017, although the distribution of urban and rural populations changes over time. Urban areas are expanding each year in China with the rapid development of urbanization; therefore, exposure risk in urban regions might be underestimated in this study. Third, the mortality rate data used to calculate the number of deaths attributable to NO_2 exposure was collected at the national level, and thus may have introduced some uncertainty. Mortality rates may vary between provincial and municipal levels due to variations among demographics and economic levels; therefore, comparisons of NO_2-related disease burdens at smaller spatial scales need to be made with great caution. Fourth, the temporal disaggregation of mortality data could not accurately reflect the potential seasonal variation of deaths and therefore may also introduce some uncertainty. Detailed mortality data could help improve the accuracy of risk assessment in the future. Last, the study failed to assess attributable deaths of cardiovascular disease (CVD) due to the lack of valid RR estimates of NO_2-CVD associations, more epidemiological studies are needed to validate the associations between NO_2 exposure and CVD to support more accurate risk assessment in the future.

5. Conclusion

In summary, based on high-resolution NO_2 predictions, we found that a large proportion of the population was exposed to NO_2 concentrations higher than the guideline levels recommended by WHO AQG 2021, and total deaths attributable to both long-term and short-term NO_2 pollution was as high as 406,299 in 2019. Our research provides new evidence to emphasize the need to strengthen air quality standards for NO_2 in China to further protect public health from NO_2 pollution.

Role of the funding source

The funder of the study had no role in study design, data collection, data analysis, data interpretation, or writing of the manuscript.

CRediT authorship contribution statement

Xinyue Li: Conceptualization, Methodology, Software, Investigation, Formal analysis, Writing – original draft, Writing – review & editing. **Peng Wang:** Data curation, Software, Validation, Writing – review & editing. **Weidong Wang:** Data curation, Validation, Software, Methodology, Writing – review & editing. **Hongliang Zhang:** Visualization, Investigation, Writing – review & editing. **Su Shi:** Resources, Writing – review & editing. **Tao Xue:** Methodology, Writing – review & editing. **Jintai Lin:** Software, Methodology, Writing – review & editing. **Yuhang Zhang:** Software, Methodology, Writing – review & editing. **Mengyao Liu:** Software, Methodology, Writing – review & editing. **Renjie Chen:** Writing – review & editing, Writing – review & editing. **Haidong Kan:** Funding acquisition, Writing – review & editing. **Xia Meng:** Conceptualization, Funding acquisition, Resources, Supervision, Writing – review & editing.

Declaration of Competing Interest

The authors declare that they have no known competing financial interests or personal relationships that could have appeared to influence the work reported in this paper.

Data availability

The data that has been used is confidential.

Acknowledgment

This work was supported by the National Key Research and Development Program of China (No. 2019YFC1804504, 2019YFC1804503), and National Natural Science Foundation of China (82003413, 92043301 and 82030103).

Appendix A. Supplementary material

Supplementary data to this article can be found online at https://doi.org/10.1016/j.envint.2023.107967.

References

Achakulwisut, P., Brauer, M., Hystad, P., Anenberg, S.C., 2019. Global, national, and urban burdens of paediatric asthma incidence attributable to ambient NO_2 pollution: estimates from global datasets. Lancet Planet Health 3, E166–E178.

Anenberg, S.C., Mohegh, A., Goldberg, D.L., Kerr, G.H., Brauer, M., Burkart, K., Hystad, P., Larkin, A., Wozniak, S., Lamsal, L., 2022. Long-term trends in urban NO_2 concentrations and associated paediatric asthma incidence: estimates from global datasets. Lancet Planet Health 6, E49–E58.

Atkinson, R.W., Butland, B.K., Anderson, H.R., Maynard, R.L., 2018. Long-term Concentrations of Nitrogen Dioxide and Mortality A Meta-analysis of Cohort Studies. Epidemiology 29, 460–472.

Bechle, M.J., Millet, D.B., Marshall, J.D., 2013. Remote sensing of exposure to NO_2: Satellite versus ground-based measurement in a large urban. Atmos. Environ. 69, 345–353.

Chen, R.J., Yin, P., Meng, X., Wang, L.J., Liu, C., Niu, Y., Lin, Z.J., Liu, Y.N., Liu, J.M., Qi, J.L., You, J.L., Kan, H.D., Zhou, M.G., 2018. Associations Between Ambient Nitrogen Dioxide and Daily Cause-specific Mortality Evidence from 272 Chinese Cities. Epidemiology 29, 482–489.

Cohen, A.J., Brauer, M., Burnett, R., Anderson, H.R., Frostad, J., Estep, K., Balakrishnan, K., Brunekreef, B., Dandona, L., Dandona, R., Feigin, V., Freedman, G., Hubbell, B., Jobling, A., Kan, H., Knibbs, L., Liu, Y., Martin, R., Morawska, L., Pope, C.A., Shin, H., Straif, K., Shaddick, G., Thomas, M., van Dingenen, R., van Donkelaar, A., Vos, T., Murray, C.J.L., Forouzanfar, M.H., 2017. Estimates and 25-year trends of the global burden of disease attributable to ambient air pollution: an analysis of data from the Global Burden of Diseases Study 2015. Lancet 389, 1907–1918.

Cyrys, J., Eeftens, M., Heinrich, J., Ampe, C., Armengaud, A., Beelen, R., Bellander, T., Beregszaszi, T., Birk, M., Cesaroni, G., Cirach, M., de Hoogh, K., De Nazelle, A., de Vocht, F., Declercq, C., Dedele, A., Dimakopoulou, K., Eriksen, K., Galassir, C., Grauleviciene, R., Grivas, G., Gruzieva, O., Gustafsson, A.H., Hoffmann, B., Iakovides, M., Ineichen, A., Kramer, U., Lanki, T., Lozano, P., Madsen, C., Meliefste, K., Modig, L., Moelter, A., Mosler, G., Nieuwenhuijsen, M., Nonnemacher, M., Oldenwening, M., Peters, A., Pontet, S., Probst-Hensch, N., Quass, U., Raaschou-Nielsen, O., Ranzi, A., Sugiri, D., Stephanou, E.G., Taimisto, P., Tsai, M.Y., Vaskovi, E., Villani, S., Wang, M., Brunekreef, B., Hoek, G., 2012. Variation of NO_2 and NO_x concentrations between and within 36 European study areas: Results from the ESCAPE study. Atmos. Environ. 62, 374–390.

Gan, T., Yang, H.C., Liang, W., Liao, X.C., 2021. Do economic development and population agglomeration inevitably aggravate haze pollution in China? New evidence from spatial econometric analysis. Environ. Sci. Pollut. R. 28, 5063–5079.

Gong, P., Li, X.C., Zhang, W., 2019a. 40-Year (1978–2017) human settlement changes in China reflected by impervious surfaces from satellite remote sensing. Sci. Bull. 64, 756–763.

Gong, P., Liu, H., Zhang, M.N., Li, C.C., Wang, J., Huang, H.B., Clinton, N., Ji, L.Y., Li, W. Y., Bai, Y.Q., Chen, B., Xu, B., Zhu, Z.L., Yuan, C., Suen, H.P., Guo, J., Xu, N., Li, W.J., Zhao, Y.Y., Yang, J., Yu, C.Q., Wang, X., Fu, H.H., Yu, L., Dronova, I., Hui, F.M., Cheng, X., Shi, X.L., Xiao, F.J., Liu, Q.F., Song, L.C., 2019b. Stable classification with limited sample: transferring a 30-m resolution sample set collected in 2015 to mapping 10-m resolution global land cover in 2017. Sci. Bull. 64, 370–373.

Guenther, A.B., Jiang, X., Heald, C.L., Sakulyanontvittaya, T., Duhl, T., Emmons, L.K., Wang, X., 2012. The Model of Emissions of Gases and Aerosols from Nature version 2.1 (MEGAN2.1): an extended and updated framework for modeling biogenic emissions. Geosci. Model Dev. 5, 1471–1492.

Gurung, A., Levy, J.I., Bell, M.L., 2017. Modeling the intraurban variation in nitrogen dioxide in urban areas in Kathmandu Valley. Nepal. Environmental Research 155, 42–48.

Huang, S.W., Li, H.M., Wang, M.R., Qian, Y.Y., Steenland, K., Caudle, W.M., Liu, Y., Sarnat, J., Papatheodorou, S., Shi, L.H., 2021. Long-term exposure to nitrogen dioxide and mortality: A systematic review and meta-analysis. Sci. Total Environ. 776.

Huang, Z., Xu, X., Ma, M., Shen, J., 2022. Assessment of NO_2 population exposure from 2005 to 2020 in China. Environ. Sci. Pollut. Res. Int.

Huangfu, P., Atkinson, R., 2020. Long-term exposure to NO_2 and O_3 and all-cause and respiratory mortality: A systematic review and meta-analysis. Environ. Int. 144, 105998.

Iqbal, A., Ahmad, N., Din, H.M.U., Van Roozendael, M., Anjum, M.S., Khan, M.Z.A., Khokhar, M.F., 2022. Retrieval of NO_2 Columns by Exploiting MAX-DOAS Observations and Comparison with OMI and TROPOMI Data during the Time Period of 2015-2019. Aerosol Air Qual Res 22.

Kaufman, J.D., Adar, S.D., Barr, R.G., Budoff, M., Burke, G.L., Curl, C.L., Daviglus, M.L., Roux, A.V.D., Gassett, A.J., Jacobs, D.R., Kronmal, R., Larson, T.V., Navas-Acien, A., Olives, C., Sampson, P.D., Sheppard, L., Siscovick, D.S., Stein, J.H., Szpiro, A.A., Watson, K.E., 2016. Association between air pollution and coronary artery calcification within six metropolitan areas in the USA (the Multi-Ethnic Study of Atherosclerosis and Air Pollution): a longitudinal cohort study. Lancet 388, 696–704.

Land Processes Distributed Active Archive Center. MODIS/Terra Vegetation Indices 16-Day L3 Global 1km SIN Grid V006. 2021.

Li, D.H., Qin, K., Cohen, J.B., He, Q., Wang, S., Li, D., Zhou, X.R., Ling, X.L., Xue, Y., 2021. Combing GOME-2B and OMI Satellite Data to Estimate Near-Surface NO_2 of Mainland China. Ieee J-Stars 14, 10269–10277.

Li, L.F., Wu, J.J., 2021. Spatiotemporal estimation of satellite-borne and ground-level NO_2 using full residual deep networks. Remote Sens. Environ. 254.

Li, M.X., Wu, Y., Bao, Y.S., Liu, B.F., Petropoulos, G.P., 2022. Near-Surface NO_2 Concentration Estimation by Random Forest Modeling and Sentinel-5P and Ancillary Data. Remote Sens-Basel 14.

Lin, J.T., Liu, M.Y., Xin, J.Y., Boersma, K.F., Spurr, R., Martin, R., Zhang, Q., 2015. Influence of aerosols and surface reflectance on satellite NO_2 retrieval: seasonal and spatial characteristics and implications for NO_x emission constraints. Atmos. Chem. Phys. 15, 11217–11241.

Liu, J.J., 2021. Mapping high resolution national daily NO_2 exposure across mainland China using an ensemble algorithm. Environ. Pollut. 279.

Liu, M.Y., Lin, J.T., Kong, H., Boersma, K.F., Eskes, H., Kanaya, Y., He, Q., Tian, X., Qin, K., Xie, P.H., Spurr, R., Ni, R.J., Yan, Y.Y., Weng, H.J., Wang, J.X., 2020. A new TROPOMI product for tropospheric NO_2 columns over East Asia with explicit aerosol corrections. Atmos. Meas. Tech. 13, 4247–4259.

Meng, X., Hang, Y., Lin, X., Li, T., Wang, T., Cao, J., Fu, Q., Dey, S., Huang, K., Liang, F., Kan, H., Shi, X., Liu, Y., 2023. A satellite-driven model to estimate long-term particulate sulfate levels and attributable mortality burden in China. Environ. Int. 171, 107740.

Meng, X., Liu, C., Chen, R.J., Sera, F., Vicedo-Cabrera, A.M., Milojevic, A., Guo, Y.M., Tong, S.L., Coelho, M.D.Z.S., Saldiva, P.H.N., Lavigne, E., Correa, P.M., Ortega, N.V., Garcia, S.O., Kysely, J., Urban, A., Orru, H., Maasikmets, M., Jaakkola, J.J.K., Ryti, N., Huber, V., Schneider, A., Katsouyanni, K., Analitis, A., Hashizume, M., Honda, Y., Ng, C.F.S., Nunes, B., Teixeira, J.P., Holobaca, I.H., Fratianni, S., Kim, H., Tobias, A., Iniguez, C., Forsberg, B., Astrom, C., Ragettli, M.S., Guo, Y.L.L., Pan, S.C., Li, S.S., Bell, M.L., Zanobetti, A., Schwartz, J., Wu, T.C., Gasparrini, A., Kan, H.D., 2021a. Short term associations of ambient nitrogen dioxide with daily total, cardiovascular, and respiratory mortality: multilocation analysis in 398 cities. Bmj-Brit Med J 372.

Meng, X.; Liu, C.; Zhang, L.; Wang, W.; Stowell, J.; Kan, H.; Liu, Y. Estimating $PM_{2.5}$ concentrations in Northeastern China with full spatiotemporal coverage, 2005-2016. Remote Sens Environ 2021b;253.

Meng, X., Wang, W.D., Shi, S., Zhu, S.Q., Wang, P., Chen, R.J., Xiao, Q.Y., Xue, T., Geng, G.N., Zhang, Q., Kan, H.D., Zhang, H.L., 2022. Evaluating the spatiotemporal ozone characteristics with high-resolution predictions in mainland China, 2013–2019. Environ. Pollut. 299.

Mills, I.C.; Atkinson, R.W.; Kang, S.; Walton, H.; Anderson, H.R. Quantitative systematic review of the associations between short-term exposure to nitrogen dioxide and mortality and hospital admissions. Bmj Open 2015;5.

Chinese Ministry of Environmental Protection, 2012. Chinese National Air Quality Standards. GB3095-2012. Ministry of Ecology and Environnment of the People's Republic of China, 2012. Governmental documents, Beijing, China.

NASA. File Specification for GEOS-5 FP (Forward Processing). 2013.

National Aeronautics and Space Administration. ASTER Global Digital Elevation Model V003. 2019.

Sannigrahi, S., Kumar, P., Molter, A., Zhang, Q., Basu, B., Basu, A.S., Pilla, F., 2021. Examining the status of improved air quality in world cities due to COVID-19 led temporary reduction in anthropogenic emissions. Environ. Res. 196.

Shen, Y., Jiang, F., Feng, S., Zheng, Y., Cai, Z., Lyu, X., 2021. Impact of weather and emission changes on NO_2 concentrations in China during 2014–2019. Environ. Pollut. 269, 116163.

Shi, S., Wang, W.D., Li, X.Y., Hang, Y., Lei, J., Kan, H.D., Meng, X., 2023. Optimizing modeling windows to better capture the long-term variation of $PM_{2.5}$ concentrations in China during 2005–2019. Sci. Total Environ. 854.

United Nations Human Settlements Programme. WORLD CITIES REPORT 2022: Envisaging the Future of Cities. 2022.

Wang, C., Wang, T., Wang, P., Rakitin, V., 2020. Comparison and Validation of TROPOMI and OMI NO_2 Observations over China. Atmos. 11, 636.

Wang, P., Ying, Q., Zhang, H., Hu, J., Lin, Y., Mao, H., 2018. Source apportionment of secondary organic aerosol in China using a regional source-oriented chemical transport model and two emission inventories. Environ. Pollut. 237, 756–766.

Wang, S.L., Li, Y.T., Hague, M., 2019. Evidence on the Impact of Winter Heating Policy on Air Pollution and Its Dynamic Changes in North China. Sustainability-Basel 11.

Wiedinmyer, C., Akagi, S.K., Yokelson, R.J., Emmons, L.K., Al-Saadi, J.A., Orlando, J.J., Soja, A.J., 2011. The Fire INventory from NCAR (FINN): a high resolution global model to estimate the emissions from open burning. Geosci. Model Dev. 4, 625–641.

World Health Organization. Air quality guidelines: global update 2005: particulate matter, ozone, nitrogen dioxide and sulfur dioxide. 2005.

World Health Organization. WHO global air quality guidelines: particulate matter ($PM_{2.5}$ and PM_{10}), ozone, nitrogen dioxide, sulfur dioxide and carbon monoxide. 2021.

Wu, H.J., Tang, X., Wang, Z.F., Wu, L., Lu, M.M., Wei, L.F., Zhu, J., 2018. Probabilistic Automatic Outlier Detection for Surface Air Quality Measurements from the China National Environmental Monitoring Network. Adv. Atmos. Sci. 35, 1522–1532.

Xiao, Q.Y., Chen, H.Y., Strickland, M.J., Kan, H.D., Chang, H.H., Klein, M., Yang, C., Meng, X., Liu, Y., 2018. Associations between birth outcomes and maternal $PM_{2.5}$ exposure in Shanghai: A comparison of three exposure assessment approaches. Environ. Int. 117, 226–236.

Xiao, Q.Y., Geng, G.N., Cheng, J., Liang, F.C., Li, R., Meng, X., Xue, T., Huang, X.M., Kan, H.D., Zhang, Q., He, K.B., 2021. Evaluation of gap-filling approaches in satellite-based daily $PM_{2.5}$ prediction models. Atmos. Environ. 244.

Xu, H.; Bechle, M.J.; Wang, M.; Szpiro, A.A.; Vedal, S.; Bai, Y.; Marshall, J.D. National $PM_{2.5}$ and NO_2 exposure models for China based on land use regression, satellite measurements, and universal kriging. Sci. Total Environ. 2019;655:423-433.

Yang, X., Zheng, Y., Geng, G., Liu, H., Man, H., Lv, Z., He, K., de Hoogh, K., 2017. Development of $PM_{2.5}$ and NO_2 models in a LUR framework incorporating satellite remote sensing and air quality model data in Pearl River Delta region, China. Environ. Pollut. 226, 143–153.

Ying, Q., Li, J., Kota, S.H., 2015. Significant Contributions of Isoprene to Summertime Secondary Organic Aerosol in Eastern United States. Environ. Sci. Tech. 49, 7834–7842.

Young, M.T., Bechle, M.J., Sampson, P.D., Szpiro, A.A., Marshall, J.D., Sheppard, L., Kaufman, J.D., 2016. Satellite-Based NO_2 and Model Validation in a National Prediction Model Based on Universal Kriging and Land-Use Regression. Environ. Sci. Tech. 50, 3686–3694.

Zhang, L.X., Guan, Y.T., Leaderer, B.P., Holford, T.R., 2013. Estimating Daily Nitrogen Dioxide Level: Exploring Traffic Effects. Ann. Appl. Stat. 7, 1763–1777.

Zhang, Z.L., Wang, J., Lu, W.J., 2018. Exposure to nitrogen dioxide and chronic obstructive pulmonary disease (COPD) in adults: a systematic review and meta-analysis. Environ. Sci. Pollut. R. 25, 15133–15145.

Zhu, Y.J., Zhan, Y., Wang, B., Li, Z., Qin, Y.Q., Zhang, K.S., 2019. Spatiotemporally mapping of the relationship between NO_2 pollution and urbanization for a megacity in Southwest China during 2005–2016. Chemosphere 220, 155–162.